Research Article

Algae 2020, 35(4): 375-388
https://doi.org/10.4490/algae.2020.35.12.8
Open Access

Effect of elevated pCO_2 on thermal performance of *Chattonella marina* and *Chattonella ovata* (Raphidophyceae)

Myeong Hwan Lim[1,2], Chung Hyeon Lee[1,2], Juhee Min[1,2], Hyun-Gwan Lee[1,2] and Kwang Young Kim[1,2,*]

[1]*Department of Oceanography, College of Natural Sciences, Chonnam National University, Gwangju 61186, Korea*
[2]*Marine Ecosystem Disturbing and Harmful Organisms (MEDHO) Research Center, Gwangju 61186, Korea*

Ocean acidification and warming, identified as environmental concerns likely to be affected by climate change, are crucial determinants of algal growth. The ichthyotoxic raphidophytes *Chattonella* species are responsible for huge economic losses and environmental impact worldwide. In this study, we investigated the impact of CO_2 on the thermal performance curves (TPCs) of *Chattonella marina* and *Chattonella ovata* grown under temperatures ranging from 13 to 34°C under ambient pCO_2 (350 µatm) and elevated pCO_2 (950 µatm). TPCs were comparable between the species or even between pCO_2 levels. With the exception of the critical thermal minimum (CT_{min}) for *C. ovata*, CT_{min} for *C. marina* and the thermal optimum (T_{opt}) and critical thermal maximum (CT_{max}) for both species did not change with elevation of pCO_2 levels. While CO_2 enrichment increased the maximum photosynthetic rates (P_{max}) up to 125% at the T_{opt} of 30°C, specific growth rates were not significantly different under elevated pCO_2 for the two species. Overall, *C. ovata* is likely to benefit from climate change, potentially widening its range of thermal tolerance limit in highly acidic waters and contributing to prolonged phenology of future phytoplankton assemblages in coastal waters.

Key Words: *Chattonella marina*; *Chattonella ovata*; growth rate; ocean acidification; photosynthetic rate; thermal performance curve; warming

INTRODUCTION

Climate change scenarios have predicted a global mean temperature rise of 2.6-4.8°C by the end of this century (Core Writing Team et al. 2014), which could affect the changes in the biogeographic range of marine species and cause a substantial pole-ward extension of biodiversity across the North Pacific (Hazen et al. 2013). Concurrently, the global average sea surface temperature (SST) has increased by 0.7°C while decreasing the pH by 0.1 units since pre-industrial times. SST is expected to rise by a further 1.2-3.2°C, and pH is expected to fall by a further 0.3-0.4 units by the year 2100 according to the Representative Concentration Pathway 8.5 (RCP8.5) (Gattuso et al. 2015). These environmental changes could affect the potentially significant role of phytoplankton in removing CO_2 from the sunlit ocean, as well as their growth and metabolism directly or indirectly in numerous ways (Raven 2017, Raven et al. 2020). Many studies have previously reported the response of marine algal growth to temperature warming and elevated CO_2 (Kremp et al. 2012, Tatters et al. 2013, Brandenburg et al. 2019, Seto et al. 2019). In general, global warming benefits algal growth if the increased temperature is below the optimal

Received October 3, 2020, **Accepted** December 8, 2020
***Corresponding Author**
E-mail: kykim@chonnam.ac.kr
Tel: +82-62-530-3465, Fax: +82-62-530-0065

temperature; beyond this temperature, it exerts adverse effects (Daufresne et al. 2009, Singh and Singh 2015). The fertilization effect of rising dissolved CO_2 concentrations in surface waters may potentially contribute to the increase in growth and production, and range expansion of many harmful algal bloom (HAB) species (Fu et al. 2012, Flynn et al. 2015, Raven 2017, Raven et al. 2020). Additional CO_2 is broadly beneficial for algal growth if nutrient availability is sufficient (Tatters et al. 2013, Thomas et al. 2017). Based on these findings, the effect of CO_2 on algal photosynthesis and growth might be more noticeable at suboptimal temperatures than at supraoptimal temperatures. However, the optimal temperature for growth will depend on the levels of dissolved inorganic carbon (DIC), as well as on numerous physiological and ecological factors (Thomas et al. 2012, Kibler et al. 2015, Brandenburg et al. 2019).

In temperate and subtropical-tropical regions of the world, the fish-killing (ichthyotoxic) raphidophytes *Chattonella* species have frequently caused serious damage to fisheries and mariculture industries in Korea (Kim et al. 2007), Japan (Imai and Yamaguchi 2012, Yamaguchi et al. 2018), China (Wang et al. 2006, 2017), North America (Lewitus et al. 2008, García-Mendoza et al. 2018), and Europe (Stacca et al. 2016, Satta et al. 2017, Zingone et al. 2020). The production of superoxide is associated with the growth of *Chattonella*, which is a strong candidate for the cause of its toxicity in fishes (Shikata et al. 2019). They inhabit the warm (~30°C) tropical waters around the equator (e.g., *Chattonella subsalsa*), extending to the colder (~5°C) waters of the Dutch Wadden Sea (e.g., *Chattonella marina* and *Chattonella antiqua*) (Vrieling et al. 1995). *Chattonella* species are often characterized by high phenotypic plasticity (Vidyarathna et al. 2020), which likely enables them to successfully colonize a wide range of environments. However, practical identification of *Chattonella* species is difficult because its pleomorphic cells and fragile nature (Coyne et al. 2005). A great morphological variability was observed as a function of laboratory culture conditions, as well as local environmental conditions; hence, there are no distinct morphological characteristics to discriminate these species (Demura et al. 2009).

Blooms of *Chattonella* tend to develop immediately after an increase in nutrient input during sunny weather and accelerate through their diel vertical migration behavior, in which cells move to the surface during the day to get access to light for photosynthesis and migrate toward the bottom during the night to have more access to nutrients throughout a diurnal cycle (Watanabe et al. 1991, Tilney et al. 2015, Shikata et al. 2019, Qiu et al. 2020). Given the potential role of resting cysts in bloom initiation of *Chattonella* species, the abundance of vegetative cells in the water column is not always relied on that of viable cysts in the sediments (Onitsuka et al. 2020). Meanwhile, the genus *Chattonella* was thought to be exclusively photosynthetic protists. However, the occurrence of mixotrophy has been described for *C. marina* and *Chattonella ovata*, which can feed on heterotrophic and autotrophic bacteria (Jeong et al. 2010, Jeong 2011). This may confer a competitive advantage to these species during nutrient shortage and add complexity to marine microbial food webs.

Chattonella species can grow over a wide range of temperatures. The appropriate temperature range for the growth of *C. marina* was from 15 to 30°C, with an optimal growth temperature of approximately 25°C (Imai and Yamaguchi 2012). The vegetative cells of *C. marina* were observed in Osaka Bay at temperatures ranging from 13 to 31°C and in the Seto Inland Sea, Japan from 18.8 to 28.0°C (Yamochi 1984, Yoshimatsu and Ono 1986). Moreover, an Australian strain of *C. marina* was able to grow at 10°C (Marshall and Hallegraeff 1999). The range of temperature have been experimentally determined for three strains of *C. ovata* isolated from Hiroshima Bay, and were found to be between 15 and 32.5°C (Yamaguchi et al. 2010). In the Seto Inland Sea, the vegetative cells of *C. ovata* found at a wide range of temperatures (15.8-31.3°C), showing the highest abundance at temperatures of 26.0-29.5°C in summer (Imai and Yamaguchi 2012). The optimal growth temperature for *C. ovata* varied between 25 and 30°C and was higher than that for *C. antiqua*, *C. marina*, and *C. subsalsa*, which showed an optimum growth temperature at 20-30°C, significantly reduced growth rates at 10-16°C, and no growth at 4°C (Kahn et al. 1998, Zhang et al. 2006, Imai and Yamaguchi 2012). The Korean strain of *C. marina* var. *marina* and *C. marina* var. *ovata* rarely grew at 10°C, and their optimal temperatures were 25 and 30°C, respectively (Noh 2009). In Korean waters, *Chattonella* species generally occur when water temperature ranges from 14.5 to 30.5°C and grow rapidly when temperature ranges from 23.1 to 30.5°C (Jeong et al. 2013). Based on these data, surface water temperature is often presumed to be a primary controlling factor for the *Chattonella* red tide in Korean waters.

The effects of temperature on fitness-related traits (i.e., photosynthesis and growth) within the survival range have been experimentally determined for a wide variety of algal species and strains (Hallegraeff 2010, Thomas et al. 2012, Kontopoulos et al. 2020). The relationship be-

tween trait rate and temperature can be visualized as a thermal performance curve (TPC). Two features of a TPC common to all ectotherms are unimodality and negative skewness (Angilletta 2006, Kingsolver 2009). The rate values increase with temperature until a critical point or optimal temperature (T_{opt}), after which they drop rapidly. The range of temperatures between maximum temperature or critical thermal maximum (CT_{max}) and the minimum temperature or critical thermal minimum (CT_{min}) is defined as the thermal niche or thermal tolerance (T_{tol}), and can vary according to an organism's phenotypic plasticity, physiological traits, and evolutionary history (Thomas et al. 2016, Jin and Agustí 2018, Vidyarathna et al. 2020). To understand the capacity for adaptation of TPC in different thermal environments, it is important to investigate how the shape of the TPC changes across species. It is also necessary to evaluate how the TPC of growth rate is affected by rising CO_2 concentration in a globally important HAB species, including *Chattonella*. However, limited information is available regarding the physiological constraints that set thermal tolerance extents in *Chattonella* species and how adaptation can overcome these constraints to enhance thermal performance. Nevertheless, this research will be essential when trying to predict the production and global distributions of *Chattonella* in the face of climate change.

The aims of this study were to determine the cardinal temperatures for the growth rate of *C. marina* and *C. ovata* under ambient and elevated CO_2 conditions from TPCs and to subsequently assess the effect of CO_2 on their photosynthesis and growth responses at the optimal growth temperature. To this end, *C. marina* and *C. ovata* were grown under two pCO_2 levels (350 and 950 µatm), in combination with five temperature (13, 20, 26, 30, and 34°C) treatments, and the interactive effects on growth rate and maximum photochemical efficiency were assessed in tightly controlled laboratory experiments.

MATERIALS AND METHODS

Cultures

The strains of two raphidophytes, *Chattonella marina* (LIMS-PS-2900) isolated from Jangmok in January 2007 and *C. ovata* (COKP9909) isolated from Gyeokpo in September 1999, were obtained from the Culture Collection of the Korea Institute of Ocean Science & Technology (KIOST) and the cultures were maintained by Prof. HJ Jeong at Seoul National University, respectively. Culture strains were grown and maintained in 250-mL Erlenmeyer flasks containing 200 mL of modified f/2 medium lacking silica at 20-23°C. The medium was prepared in sterilized natural seawater, with a salinity of 32-34 at pH 8.0. A 12 : 12 h light-dark cycle with 120-150 µmol photons m^{-2} s^{-1} light intensity was provided by 36 W daylight fluorescent lamps (Dulux L 36W/865; Osram, Mu¨nich, Germany). Cultures were transferred weekly to keep them in exponential growth phase until the start of the experiment.

Experimental setup

C. marina and *C. ovata* were semi-continuously cultured for 7 days after a 3-day batch culture under each treatment condition (see below). During the semi-continuous culture, Erlenmeyer flasks (100 mL capacity) containing 100 mL of cultures were kept at the lower section of the exponential growth phase (Supplementary Fig. S1) and were optically thin to avoid self-shading, nutrient limitation, and to minimize CO_2 drift. The culture flasks were shaken gently twice a day to ensure the mixing of cell suspensions. The five temperature levels (13, 18, 25, 30, and 34°C) were combined with two CO_2 partial pressures (pCO_2); 350 µatm (ambient pCO_2 treatment) or 950 µatm (elevated pCO_2 or ocean acidification [OA] treatment), and experiments were performed in triplicate. These OA mimicking values were based on the IPCC WG RCP 8.5 scenario. Every 24 h, the cultures were diluted with the respective f/2 media that had been adjusted to the two target pCO_2 levels, to a starting cell concentration of 100 cells mL^{-1} in *C. marina* and 400 cells mL^{-1} in *C. ovata*. To attain and maintain the target pCO_2 or pH values, the culture was additionally adjusted by adding an appropriate amount of CO_2-saturated seawater. No more than 10 µL of CO_2-saturated seawater was used. CO_2-saturated seawater was prepared by bubbling reagent-grade CO_2 through seawater within gas tight containers, which caused the medium pH to drop below 5. Prior to every dilution, 5 mL of culture were collected in triplicate from semi-continuous cultures to measure photosynthetic efficiency, spectrophotometric pH (total scale), and cell counts.

Temperature gradients

The five target temperatures, ranging from 13 to 34°C were obtained using a plexiglass aquarium (45 cm × 20 cm × 20 cm) with a thermostatically controlled water bath, filled with deionized water and equipped with a heater and a cooler, which allowed control of the tem-

perature with a precision of ±0.3°C (Supplementary Fig. S1). The temperature inside the aquarium was logged every 30 min using a HOBO temperature logging device (Onset Computer Corporation, Pocasset, MA, USA). Erlenmeyer flasks (100 mL capacity) containing 100 mL of culture were placed in a plexiglass aquarium in three replicates, under 120 µmol photons m^{-2} s^{-1} of photosynthetically active radiation (400-700 nm) with a 14 : 10 h light-dark cycle.

Inorganic carbon chemistry

The inorganic carbon chemistry was determined using the CO2SYS program (Lewis and Wallace 1998) using total alkalinity (A_T), total pH scale, salinity, and temperature of culture seawater. The A_T was measured using potentiometric acid titration in a semi-closed cell system, consisting of a Metrohm 765 Dosimat titrator (Metrohm, Zofingen, Switzerland) connected to a pH meter (Orion 920A; Thermo Fisher Scientific, Waltham, MA, USA). The added volume of acid (0.13 N HCl) and electromotive force were recorded using Q-basic software during each titration (Millero et al. 1993). The pH of the culture samples was determined using a high-resolution spectrophotometer (Agilent 8453, UV-VIS Spectrophotometer; Agilent Technologies, Palo Alto, CA, USA). Absorbance at wavelengths of 434, 578, and 730 nm of seawater samples were measured at 25°C with m-cresol purple indicator dye (Sigma-Aldrich Chemical Co., St. Louis, MO, USA) (Dickson 1993). The method employed was essentially the same as that described by Kim et al. (2018).

Maximum photochemical efficiency of photosystem II

The photosynthetic activity of *Chattonella* cultures was determined using pulse amplitude-modulated (PAM) chlorophyll-*a* fluorometry (Phyto-PAM fluorometer; Walz GmbH, Effeltrich, Germany). The maximum efficiency of photosystem II (PSII) photochemistry (F_v/F_m) was measured for each culture after being acclimatized to darkness for 10 min, where F_v (variable fluorescence) is calculated as the difference between F_m and F_o fluorescence, F_o is the fluorescence level in the absence of actinic (photosynthetic) light for open PSII reaction centers, and F_m is the maximum fluorescence at closed reaction centers induced by a short pulse of saturating light (Genty et al. 1989).

Photosynthesis vs. irradiance curves (*P-E* curves)

Photosynthetic oxygen evolution was measured by inserting a Clark-type O_2 microelectrode with a tip diameter of 500 µm (OX-MR; Unisense, Aarhus, Denmark) connected to a pico-amperemeter (PA2000; Unisense) into a 4 mL micro-respiration chamber (Unisense) in a thermostatically controlled water bath at 30°C. The O_2 concentration of cultures was recorded every minute for 15-20 min at all light intensities. The oxygen electrode was two-point calibrated by measuring between 0 and 100% saturated seawater. A 250 W halogen lamp (KL 2500 LCD; Schott, Mainz, Germany) illuminated the setup, and variable levels of irradiance were obtained by using shade screens with different densities (0, 21, 42, 80, 171, 326, and 652 µmol photons m^{-2} s^{-1}). Real-time oxygen measurements were initiated by measuring respiration in darkness. Photosynthesis was subsequently measured at increasing levels of irradiance. Rates of O_2 consumption or release were calculated from incubation periods with constant changes in O_2 concentration over a minimum of 10 min. A full photosynthesis-irradiance (*P-E*) curve for each sample lasted for 2-3 h, and three replicate *P-E* curves were run. Photosynthetic rates were expressed in units of µmol O_2 $cell^{-1}$ d^{-1}. The photosynthetic parameters of the *P-E* curves were estimated by the nonlinear regression model of Platt et al. (1980) to identify photosynthetic traits. The maximum photosynthetic rate in the absence of photoinhibition (P_{max}, µmol O_2 $cell^{-1}$ h^{-1}), photosynthetic efficiency under non-saturating irradiance or the initial slope of the *P-E* curve (α, µmol O_2 $cell^{-1}$ h^{-1} [µmol photons m^{-2} s^{-1}]$^{-1}$), and irradiance at onset of saturation for *P-I* curves or light-saturation parameter (E_k, µmol photons m^{-2} s^{-1}) were determined using the least squares curve fitting technique included with the software Grapher ver. 12 (Golden Software Inc., Golden, CO, USA).

Growth

The number of live cell was counted daily in a 1 mL Sedgewick-Rafter counting chamber under a compound microscope. If there was not enough time for this task, samples were preserved with 5% Lugol's iodine solution for later enumeration. Growth was calculated as the specific growth rate (μ d^{-1}) as follows:

$$\mu = \ln (N_t - N_0) / \Delta t$$

, where N_0 and N_t denote the cell concentration at the ini-

tial and after a time interval of the experiments, and Δt is the corresponding incubation time (d) of exponential growth (Supplementary Figs S2 & S3).

Cardinal temperature estimation

The growth-temperature (μ-T) curves were described by fitting the cardinal temperature model with inflection (CTMI) described by Rosso et al. (1993):

$$\mu_{max} = \mu_{opt}\{(T - CT_{max})(T - CT_{min})^2 / (T_{opt} - CT_{min})[(T_{opt} - CT_{min})(T - T_{opt}) - (T_{opt} - CT_{max})(T_{opt} + CT_{min} - 2T)]\}$$

for $T_{min} \leq T \leq T_{max}$, where T is the temperature (°C), μ is the specific growth rate on d^{-1}, T_{opt} is the optimal temperature at which the specific growth rate is maximal, and μ_{opt} is the specific growth rate at T_{opt}. CT_{min} and CT_{max} are the hypothetical lower and upper critical temperature (critical thermal minimum and maximum), respectively, through which the specific growth rate is zero. Because an estimation of CT_{max} and CT_{max} at zero has limited biological meaning, we calculated CT_{min} and CT_{max} as the temperatures at which performance was 5% of the maximum performance. The range between CT_{min} and CT_{max} is termed the tolerance range (T_{tol}). The thermal performance breadth (TB_{80}) was also determined and was defined as the temperature range through which the growth rate was close to optimal (defined as the 80th percentile of the CTMI fits).

Statistical analyses

The main and combined effects of two pCO_2 (ambient and elevated) and five temperature treatments with respect to all experimental parameters (carbonate chemistry, growth rate, and maximum efficiency of PSII photochemistry) were evaluated by two-way analyses of variance (ANOVAs). Prior to the statistical analysis, data sets were tested for conformity to normality and for homogeneity of variances using the Shapiro-Wilk and Levene's test, respectively. Two-way ANOVA was also performed to determine the effects of pCO_2 on species and their interaction based on the photosynthetic and growth rates at the optimal growth temperature (30°C). If a significant ANOVA was found, differences among the group means were tested using Scheffé's post hoc tests

Table 1. A summary of the seawater carbon chemistry of the *Chattonella marina* and *C. ovata* cultures at two target pCO_2 (350 and 950 µatm) and five temperatures (13, 20, 26, 30, and 34°C) during the experiment

Treatment		pH *in situ*	pCO_2 (µatm)	HCO_3^- (µmol kg^{-1})	CO_3^{2-} (µmol kg^{-1})	CO_2 (µmol kg^{-1})
Temperature (°C)	pCO_2 (µatm)					
C. marina						
13	350	7.95 ± 0.13^{b}	531.6 ± 162.2^{B}	$1{,}991.8 \pm 83.3^{\beta}$	126.2 ± 33.7^{iii}	21.2 ± 6.5^{II}
	950	7.68 ± 0.07^{d}	$1{,}065.4 \pm 164.5^{E}$	$2{,}097.3 \pm 34.5^{\delta}$	107.3 ± 14.1^{iv}	30.9 ± 4.4^{V}
20	350	8.08 ± 0.06^{a}	360.4 ± 59.3^{A}	$1{,}745.6 \pm 56.2^{\alpha}$	226.9 ± 22.8^{i}	10.3 ± 1.7^{I}
	950	7.71 ± 0.06^{cd}	$1{,}005.9 \pm 146.9^{DE}$	$2{,}073.8 \pm 34.9^{\delta}$	113.6 ± 14.3^{iv}	$28.8 \pm 4.0^{IV\ V}$
26	350	8.08 ± 0.06^{a}	361.3 ± 60.0^{A}	$1{,}747.3 \pm 54.3^{\alpha}$	226.8 ± 22.1^{i}	10.3 ± 1.7^{I}
	950	7.72 ± 0.07^{cd}	960.3 ± 164.0^{CD}	$2{,}037.1 \pm 40.0^{\gamma}$	$121.5 \pm 16.4^{iii\ iv}$	$26.6 \pm 4.4^{III\ IV}$
30	350	8.08 ± 0.05^{a}	362.1 ± 56.6^{A}	$1{,}751.9 \pm 53.4^{\alpha}$	227.1 ± 21.7^{i}	10.3 ± 1.6^{I}
	950	7.75 ± 0.06^{c}	906.3 ± 148.5^{C}	$2{,}035.9 \pm 37.8^{\gamma}$	129.4 ± 15.5^{iii}	25.0 ± 3.8^{III}
34	350	8.00 ± 0.04^{b}	453.1 ± 48.8^{B}	$1{,}828.7 \pm 33.3^{\beta}$	196.2 ± 13.5^{ii}	12.9 ± 1.4^{I}
	950	7.75 ± 0.06^{c}	895.7 ± 139.3^{C}	$2{,}035.9 \pm 41.0^{\gamma}$	129.0 ± 16.9^{iii}	25.1 ± 4.7^{III}
C. ovata						
13	350	8.12 ± 0.08^{ab}	321.6 ± 71.4^{A}	$1{,}700.2 \pm 70.1^{\beta\gamma}$	227.0 ± 28.3^{ii}	9.6 ± 2.1^{I}
	950	7.67 ± 0.03^{d}	$1{,}060.5 \pm 83.0^{C}$	$2{,}034.2 \pm 8.4^{\varepsilon}$	96.0 ± 3.4^{iv}	31.5 ± 1.6^{III}
20	350	8.16 ± 0.06^{a}	279.3 ± 51.9^{A}	$1{,}655.3 \pm 62.4^{\alpha\beta}$	248.4 ± 25.3^{i}	8.3 ± 1.5^{I}
	950	7.69 ± 0.05^{cd}	998.3 ± 139.2^{C}	$2{,}012.0 \pm 25.0^{\delta\varepsilon}$	$103.7 \pm 10.2^{iii\ iv}$	29.2 ± 4.1^{III}
26	350	8.15 ± 0.07^{a}	295.6 ± 66.4^{A}	$1{,}665.5 \pm 78.5^{\alpha\beta}$	246.0 ± 31.8^{i}	8.6 ± 2.0^{I}
	950	7.73 ± 0.05^{c}	906.7 ± 116.2^{B}	$1{,}989.5 \pm 32.7^{\delta\varepsilon}$	$114.4 \pm 13.4^{iii\ iv}$	26.2 ± 3.5^{II}
30	350	8.16 ± 0.04^{a}	277.1 ± 30.6^{A}	$1{,}642.4 \pm 40.6^{\alpha}$	254.5 ± 16.4^{i}	8.0 ± 0.9^{I}
	950	7.73 ± 0.05^{c}	898.0 ± 123.9^{B}	$1{,}982.5 \pm 34.0^{\delta}$	116.4 ± 13.9^{iii}	25.7 ± 3.6^{II}
34	350	8.09 ± 0.05^{b}	339.8 ± 53.8^{A}	$1{,}709.2 \pm 55.4^{\gamma}$	227.9 ± 22.5^{ii}	9.8 ± 1.7^{I}
	950	7.73 ± 0.05^{c}	900.6 ± 101.4^{B}	$1{,}987.4 \pm 28.2^{\delta}$	116.7 ± 11.5^{iii}	25.7 ± 3.0^{II}

Data are mean ± standard deviation (n = 33-39) in each treatment.

Inorganic carbon parameters, which were not directly measured, were calculated using the CO2SYS program (Lewis and Wallace 1998) using total alkalinity (A_T), total pH scale, salinity, and temperature. Different letters represent significant differences (Scheffé's test after ANOVA, $p < 0.05$) between pCO_2 treatments within the same column.

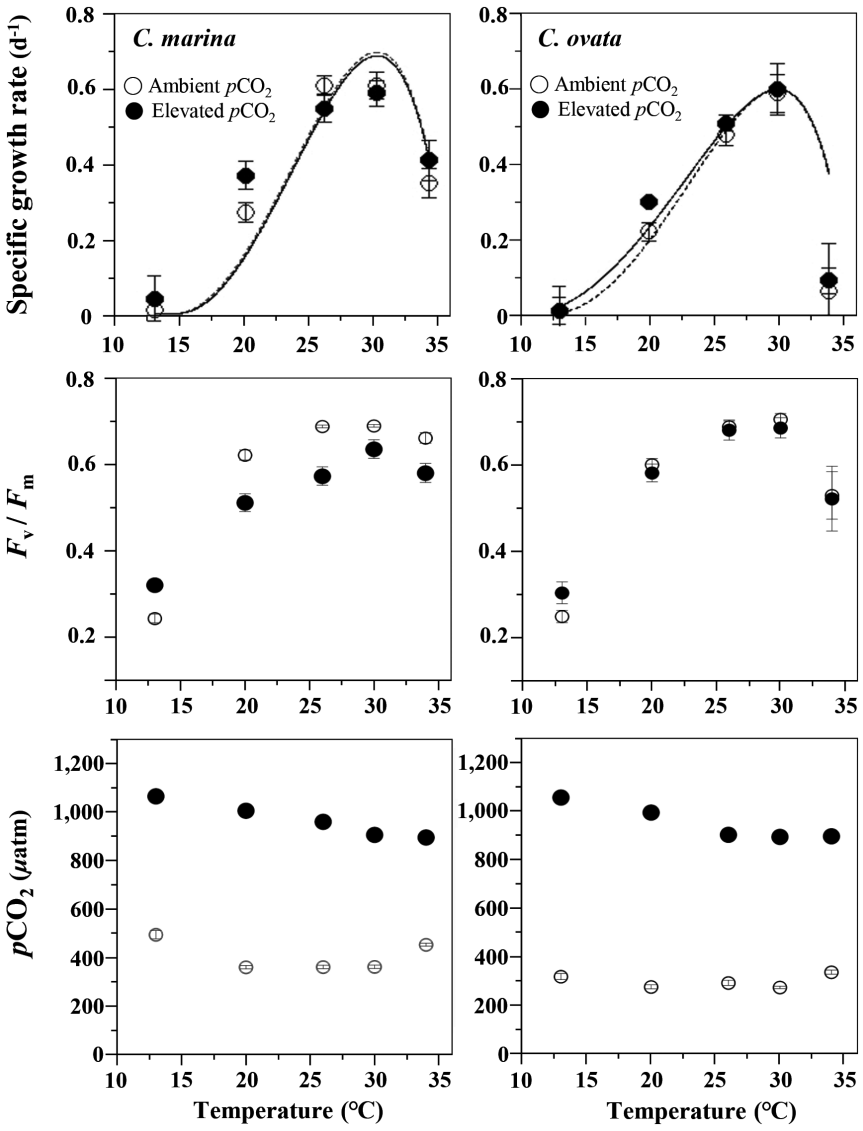

Fig. 1. Specific growth rate (μ d^{-1}) and maximum photochemical efficiency (F_v/F_m) of *Chattonella marina* and *C. ovata* in response to pCO_2 and water temperature treatments. Vertical bars indicate the mean ± standard error (n = 3) for ambient (open circles) and elevated (filled circles) pCO_2 treatments. Lines represent the best fit of the data to the Cardinal Temperature Model with Inflection (CTMI) model of Rosso et al. (1993) with r^2 of 0.959 (open circles) and 0.918 (filled circles) in *C. marina*, and 0.876 (open circles) and 0.805 (filed circles) in *C. ovata*.

for multiple comparisons. All statistical analyses were performed using SPSS Statistics ver. 25 (IBM Corp., Armonk, NY, USA).

RESULTS

The two target pCO_2 levels 350 and 950 µatm were successfully maintained at all temperature treatments throughout the experimental period (Table 1). Regardless of temperature, the pCO_2 (mean ± standard deviation) in cultures of *C. marina* was significantly higher under elevated pCO_2 (966.7 ± 164.6, n = 300) than under ambient pCO_2 (413.5 ± 112.6, n = 366) (Scheffé's test after ANOVA; $p < 0.001$). The pCO_2 of *C. ovata* cultures was also significantly higher under elevated pCO_2 (946.2 ± 130.5, n = 192) than under ambient pCO_2 conditions (302.7 ± 61.6, n = 189) (Scheffé's test after ANOVA; $p < 0.001$) at all five temperature treatments. Similar trends for the pCO_2 were apparent for the pH values, which showed a range of 7.80 to 8.24 and 7.59 to 7.91 in cultures of *C. marina* of ambient and elevated pCO_2 levels, respectively. The pH

in cultures of *C. ovata* was also significantly lower under elevated than under ambient pCO_2 levels (Scheffé's test after ANOVA; $p < 0.001$), with ranges between 7.93 to 8.27 and 7.56 to 7.87, respectively (Table 1). In addition, the concentrations of bicarbonate (HCO_3^-) increased significantly with decreasing pH, whereas carbonate (CO_3^{2-}) decreased under elevated pCO_2 conditions. On the initial and final day of the experiment, total alkalinity (A_T, μmol kg^{-1}) remained constant with average and standard deviation values of 2,331.2 ± 15.3 (n = 6) and 2,318.2 ± 11.17 (n = 30) in the cultures of *C. marina*, and 2,260.6 ± 5.0 (n = 6) and 2,273.2 ± 6.6 (n = 30) in the cultures of *C. ovata*, respectively.

The specific growth rate (μ) was similar between *C. marina* and *C. ovata*, both at the ambient and elevated pCO_2 (Fig. 1, upper panel). They grew over a wide range of temperatures (13-34°C), with optimum growth temperatures around 30°C under both pCO_2 treatments. Cultures grown under elevated pCO_2 exhibited an average increase of 6% in growth rates of *C. ovata* only, compared with those grown under ambient pCO_2 across temperature treatments. Cultures of *C. marina* grown at 13°C showed the lowest growth rates, whereas cultures maintained at 34°C had the highest growth rate. The growth rate of increase in *C. ovata* with temperature increased to 30°C and then decreased abruptly at 34°C, maintaining only 10-15% of the maximum growth rate. ANOVA demonstrated that the specific growth rates of *C. marina* and *C. ovata* grow under two pCO_2 levels over a range of temperatures, were significantly affected by temperature (df = 4, F = 77.3, $p < 0.001$ for *C. marina*; df = 4, F = 110.2, $p < 0.001$ for *C. ovata*), but not by either pCO_2 treatments or pCO_2 and temperature interaction. Scheffé's post hoc analysis revealed significant differences between the growth rate at the lowest temperature (13°C) and those at the other temperatures for *C. marina* ($p < 0.001$). There were also significant differences in growth rates of *C. ovata* at 13 and 34°C compared with those at the rest of the temperatures examined ($p < 0.001$). Noticeably, the growth rates of *C. ovata* in the range of temperatures below the optimal were slightly higher at elevated pCO_2 than ambient pCO_2 treatments.

Unlike growth rate, the maximum photochemical efficiency (F_v/F_m) of *C. marina* and *C. ovata* increased under both pCO_2 levels as temperatures increased from 13 to 30°C, showing the capacity to maintain photosynthesis at 34°C (Fig. 1, middle panel). The F_v/F_m was greatest at the optimal growth temperature under both pCO_2 conditions, and exhibited similar trends in both species, with cultures receiving the 20, 26, 30, and 34°C treatments, producing 0.5-0.7, except at 13°C (Fig. 1, middle panel, Supplementary Fig. S4). Both temperature and pCO_2 treatments had significant effect on the F_v/F_m of *C. marina* cultures (df = 4, F = 234.4, $p < 0.001$ for temperature; df = 1, F = 39.0, $p < 0.001$ for pCO_2). In addition, an interaction effect of temperature and pCO_2 on the F_v/F_m of *C. marina* was observed (df = 4, F = 15.2, $p < 0.001$). For *C. ovata*, only the temperature significantly influenced the F_v/F_m (df = 3, F = 259.8, $p < 0.001$). In both pCO_2 conditions, Scheffé's post hoc tests showed that F_v/F_m value at 13°C was significantly lower ($p < 0.001$) compared to that at the other temperatures.

Application of CTMI model to the growth rate resulted in cardinal temperatures, that is critical thermal minimum (CT_{min}), critical thermal maximum (CT_{max}), thermal optimum or optimal temperature (T_{opt}). Under ambient pCO_2 conditions, the CT_{min}, CT_{max}, and T_{opt} for the growth rate of *C. marina* were estimated to be 17.0, 35.6, and 30.0°C, respectively. Under elevated pCO_2 conditions, the CT_{min}, CT_{max}, and T_{opt} were estimated to be 17.1, 35.7, and 30.0°C, respectively (Table 2). Using the CTMI model, the CT_{min}, CT_{max}, and T_{opt} for the growth rate of *C. ovata* under ambient pCO_2 conditions were estimated to be 15.1, 35.7, and 30.0°C, respectively. Under elevated pCO_2 conditions, a CT_{min} of 13.6, CT_{max} of 35.7, and T_{opt} of 30.0°C were obtained (Table 2). Overall, there was only a slight decrease in the CT_{min} in response to elevated pCO_2, but no change in either CT_{max} and T_{opt} between the ambient and elevated pCO_2 treatments.

A more comprehensive assessment of the light-dependence of photosynthesis or oxygen evolution rate was performed at the optimal growth temperature of 30°C (Fig. 2). The photosynthetic efficiency under non-saturating irradiance or initial slope (α) of the *P-E* curve showed little response to pCO_2, but the maximum pho-

Table 2. Parameters of thermal performance curve for the growth rate of *Chattonella marina* and *C. ovata* in response to pCO_2 (ambient 350 and elevated 950 μatm), as calculated by the CTMI (Cardinal Temperature Model with Inflection) model

Parameter	CT_{min}	CT_{max}	T_{opt}	μ_{max}	T_{tol}	TB_{80}
C. marina						
Ambient pCO_2	17.0	35.6	30.0	0.70	18.6	6.8
Elevated pCO_2	17.1	35.7	30.0	0.69	18.6	6.8
C. ovata						
Ambient pCO_2	15.1	35.7	30.0	0.60	20.6	7.3
Elevated pCO_2	13.6	35.7	30.0	0.60	22.1	7.6

CT_{min}, critical thermal minimum; CT_{max}, critical thermal maximum; T_{opt}, thermal optimum or optimal temperature; μ_{max}, maximum performance or maximum growth rate; T_{tol}, thermal tolerance; TB_{80}, thermal performance breadth.

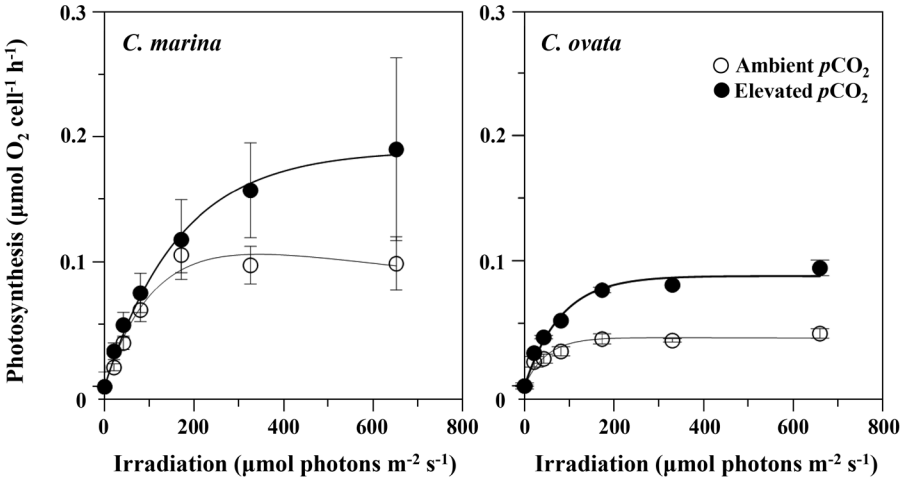

Fig. 2. Effect of elevated pCO_2 on gross photosynthesis or oxygen evolution rates of *Chattonella marina* and *C. ovata* in response to photosynthetic photon flux density at optimal growth temperature (30°C). Vertical bars indicate the mean ± standard error (n = 3) for ambient (open circles) and elevated (filled circles) pCO_2 levels. Lines represent the best fit of the data to the photoinhibition model of Platt et al. (1980).

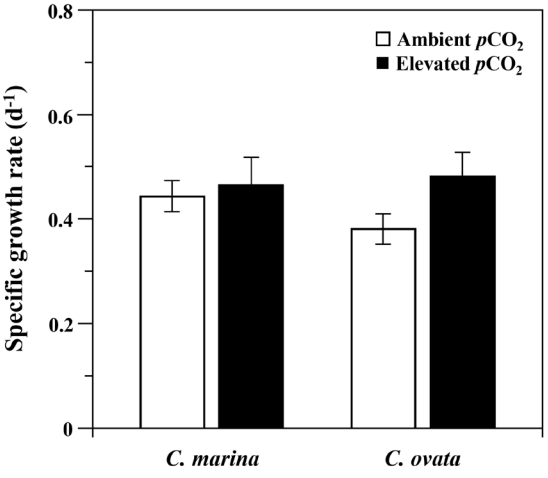

Fig. 3. Specific growth rate (μ d^{-1}) of *Chattonella marina* and *C. ovata* at optimal growth temperature (30°C). Vertical bars indicate the mean ± standard error (n = 3) for ambient (open column) and elevated (filled column) pCO_2 levels. None of the differences were statistically significant by two-way ANOVA (p > 0.001).

tosynthetic rate (P_{max}) increased by 78% from 0.106 µmol O_2 cell^{-1} h^{-1} at ambient conditions to 0.189 µmol O_2 cell^{-1} h^{-1} at elevated pCO_2 levels for *C. marina*. A corresponding increase by 125%, from 0.039 to 0.088 µmol O_2 cell^{-1} h^{-1}, was seen in *C. ovata*. The photosynthetic photon flux density at which the highest photosynthetic rate (E_k) occurred also increased with pCO_2 levels from 96 µmol photons m^{-2} s^{-1} at ambient pCO_2 to 171 µmol photons m^{-2} s^{-1} at the elevated pCO_2 for *C. marina*. The light-saturation parameter (E_k) for *C. ovata* showed a similar response to pCO_2, but was much lower than that of *C. marina*.

All measured growth rates at the optimal growth temperature (30°C) were generally similar between the CO_2 treatments (Fig. 3). Analysis of the growth rate as a function of pCO_2 indicated that it was not changed by increasing CO_2, and only a small difference was found between the two species (Fig. 3). For *C. marina*, the mean growth rates at ambient and elevated pCO_2 were 0.44 ± 0.03 and 0.47 ± 0.03, respectively, while the comparable values for *C. ovata* were 0.38 ± 0.05 and 0.48 ± 0.04, respectively. The two species did not differ significantly in response of specific growth rate to pCO_2 (df = 1, F = 0.351, p = 0.578). The growth rates of both species exposed to elevated pCO_2 were slightly greater than those exposed to ambient conditions, but the difference was not significant (df = 1, F = 2.379, p = 0.133). In addition, the interaction between the CO_2 concentration and the species was not statistically significant (df = 1, F = 0.871, p = 0.358).

Our key findings for *Chattonella* were as follows: (1) the maximum performance or maximum growth rate (μ_{max}) was slightly higher in *C. marina* than in *C. ovata*; (2) thermal tolerance (T_{tol}) and thermal performance breadth (TB_{80}) were slightly greater in *C. ovata* than in *C. marina*; (3) CO_2 affected the T_{tol} and TB_{80} in *C. ovata* but not in *C. marina*; (4) at the optimal temperature (T_{opt}), CO_2 affected the maximum photosynthetic rate (P_{max}), but there was no effect of CO_2 on the specific growth rate (μ) in both species.

DISCUSSION

Chattonella marina var. *ovata* strains from Korea rarely grew at 10°C, and slightly at 15°C, with growth increasing to a maximum of 0.62 d^{-1} at 30°C (Noh 2009). *C. marina* var. *marina* showed a pattern similar to that of *C. marina* var. *ovata*, although its peak growth rate was 0.64 d^{-1} at 25°C (Noh 2009). In Korean waters, *Chattonella* species were identified when the water temperature was 14.5-30.5°C, and the water temperature during *Chattonella* red tides was 23.1-30.5°C (Jeong et al. 2013). These species were also found at 10-33°C in the waters of other countries and formed red tides at 24.0-31.0°C (see Jeong et al. 2013, table 4). Therefore, *Chattonella* occurrence and bloom dynamics are likely to respond similarly to water temperature in Korean waters as in the waters of other countries.

To better predict how species respond to changes in temperature, it is necessary to depict the shape of TPC (Kontopoulos et al. 2020). TPCs describe an organism's eco-physiological trait according to temperature, which generally has a concave unimodal shape. The shape of TPC is similar across taxa, and much of the variation can be attributed to several factors, including genetics, seasonal, latitudinal, or acclimation capacity (Kingsolver 2009, Clusella-Trullas et al. 2011, Boyd et al. 2013, Bernhardt et al. 2018). In our results, all TPCs were non-symmetrical around the optimal temperature (30°C), exhibiting negative skewness. The curves exhibited a sudden sharp decline in growth rate accompanying small changes in temperature closer to the upper tolerance limit, and a smaller change in growth rate with changes in temperature near the lower limit (Fig. 1, upper panel). This indicates that when acclimated to T_{opt}, fitness-related traits (i.e., photosynthesis and growth) are more significantly reduced by warming than cooling. Other research has suggested that OA has great potential to increase phytoplankton growth rates in regions of the ocean where temperature is equal to or less than the T_{opt} (Boatman et al. 2017). Considering the SST anomaly from KNIFS (Korean National Institute of Fisheries Science) and the T_{opt} of 30°C estimated for two *Chattonella* species in the present results, future warming is likely and will contribute to further intense, more frequent, and longer *Chattonella* red tides in Korean waters.

In a previous study, laboratory experiments and meta-analyses were conducted using TPCs to understand the differences in functional traits and physiological responses to temperature between phytoplankton species and between strains (Boyd et al. 2013). The CTMI model is derived from the prediction of a specific growth rate as a function of temperature in species or strains on the basis of empirical knowledge of cardinal temperatures and best visual fit, with respect to the available data (Rosso et al. 1995). In this study, the cardinal temperature parameters were calculated using the CTMI model for each *Chattonella* species and CO_2 treatment to describe the growth rate change, including the biological significance obtained at different temperatures (Fig. 1, upper panel). Two other essential parameters derived from TPCs are thermal tolerance ($T_{tol} = CT_{max} - CT_{min}$) and thermal performance breadth (TB_{80}). TB_{80} is the range of water temperatures over which the performance is greater than a given proportion (80%) of μ_{max} (e.g., TB_{80} = 80% of μ_{max}) (Angilletta 2006). Because cultures are likely to continue to be active at temperatures beyond T_{opt}, TB_{80} represents the temperature range where cultures exhibit ≥80% of their maximal growth rate or performance, providing a conservative optimal performance range beyond which cultures begin to lose the ability to grow. Cardinal temperatures by CO_2 interactions have been observed for only *C. ovata*, and there are slight increases in T_{tol} and TB_{80} to elevated CO_2 without increasing growth rate (Table 2). Temperatures above TB_{80} result in steep decreases in performance until cultures become non-active, corresponding with the CT_{max}. The maximum temperature limit for growth or CT_{max} was similar between the two species and the two CO_2 treatments. How future increases in surface temperature will influence the distribution will depend on the capacity for *Chattonella* species to adapt by increasing its CT_{max} or upper thermal tolerance limit. Interestingly, we found that *C. marina* and *C. ovata* have 5°C higher CT_{max} values than that did *C. marina* or *C. Antiqua* (Noh 2009, Imai and Yamaguchi 2012). There were no differences in CT_{max} and T_{opt} between species or CO_2 treatments, with values of 35.7 and 30.0°C, respectively (Table 2). However, T_{tol} and TB_{80} depend on species and CO_2 treatments in *C. ovata*; specifically, the effect of the CO_2 on growth of *C. ovata* was more pronounced at suboptimal than supraoptimal temperatures. Although no change in the CT_{min} of 17°C for *C. marina*, the CT_{min} for *C. ovata* growth was affected by CO_2 and dropped from 15.1°C at ambient to 13.6°C at elevated CO_2. The drop in CT_{min} with CO_2 enrichment may even be underestimated, as it represents the temperature at which the growth rate exhibits ≤5% of the maximum performance. The thermal tolerance or niche showed a relatively wide temperature range from 17.0-35.7°C in *C. marina* and 13.6-35.7°C in *C. ovata*, is a key factor that sets the limits of their geographic distribution. Therefore, the parameters of TPC

for growth rate extracted from each species-specific fit are necessary to better predict the impact of future climate change on large-scale biogeographic patterns in marine systems (Bestion et al. 2018, Kontopoulos et al. 2020).

Under light-saturated conditions, the maximum photochemical efficiency (F_v/F_m) peaked near T_{opt} and remained high at temperatures above T_{opt}, indicating that PSII was not damaged by high temperatures, irrespective of pCO_2. The target sites of elevated temperature-induced or thermal damage in plants are the oxygen-evolving complex with the associated cofactors in PSII, the carboxylation activity of ribulose bisphosphate carboxylase-oxygenase (Rubisco), and the ATP generating system (Allakhverdiev et al. 2008). The photosynthetic rate of algae is limited by the activity of Rubisco, which in turn is influenced by various environmental factors, including light, temperature, nutrients, and DIC. Inorganic carbon acquisition strategies are likely to vary among species, due to differences in the operation of their carbon concentrating mechanisms (CCMs), which maintain elevated CO_2 concentrations in the vicinity of Rubsco to ensure effective carboxylation and, consequently, efficient carbon fixation (Thoms et al. 2001, Giordano et al. 2005). The current CO_2 concentrations are insufficient to saturate Rubisco carboxylation activity through passive CO_2 diffusion into the cell in eukaryotic algae (Tortell et al. 2000, Beardall et al. 2009). Under such carbon-limited conditions, marine algae that utilize HCO_3^-, or rely on active CO_2 uptake, could benefit from higher pCO_2 by downregulating their CCMs, as such CCMs have high energy demands (Rost et al. 2008, Beardall et al. 2009, Eberlein et al. 2016, Van de Waal et al. 2019). Consequently, an increase in DIC availability in the water will result in a rise in photosynthetic rate and subsequent growth, in part because high CO_2 concentrations inhibit the oxygenase reaction of Rubisco and reduce the loss of CO_2 through photorespiration.

While the DIC was significantly higher in elevated pCO_2 relative to the ambient pCO_2 treatments, the carbonate chemistry in both species cultures significantly differed between the ambient and elevated pCO_2 conditions (Table 1). Specifically, the pH decreased by 0.24-0.45 units relative to the ambient pH when the pCO_2 level was elevated by appropriate injection of CO_2-saturated seawater. As a consequence, the process made it possible to maintain carbonate chemistry throughout the entire experimental period. There are changes in carbonate system speciation; increasing pCO_2 (which is equivalent to increasing DIC at constant A_T) leads to an increase in H^+ (decreasing pH) and bicarbonate (HCO_3^-) concentrations and decreasing carbonate (CO_3^{2-}) concentrations (Table 1). There are two basic experimental approaches to adjust seawater CO_2; either changing total alkalinity (A_T) at constant DIC by NaOH and / or HCl addition or changing DIC at constant A_T (e.g., aeration with air at target pCO_2, injection of CO_2-saturated seawater, combined $NaHCO_3$ / Na_2CO_3 and HCl additions) (Gattuso et al. 2010). Experimentally, DIC or A_T can be manipulated in different ways, depending on whether the initial seawater values are lower or higher than intended. While A_T can be manipulated by adding strong acids or bases such as HCl or NaOH, various methods exist to increase or decrease pCO_2 or DIC. In this study, the target pCO_2 or DIC can be adjusted by injection of certain amounts of CO_2-saturated seawater, which can easily be prepared by aeration with pure CO_2 gas. Naturally occurring anthropogenic CO_2 intrusion of the surface ocean increases seawater pCO_2 and DIC without changing A_T. Again, A_T is not influenced by CO_2 uptake and remains constant (Schulz et al. 2009). Furthermore, the unarmored and fragile cell nature of *Chattonella* are sensitive to the physical stresses, and the gas bubbles produced by aeration with air at the target pCO_2 seem to be the cause of cell damage or breakage.

Despite different growth responses in different HAB species to high CO_2, a number of HABs have generally been shown to experience increased growth rates under elevated CO_2 concentrations; however, some other studies showed no increase in growth rate with pCO_2 above the present air-equilibrium concentration. Even different isolates within a given species may have opposite responses to high and low CO_2 for eukaryotic species (see Raven et al. 2020). It seems that different HABs differ in their capacity and strategy to adjust metabolism to high CO_2 conditions. Furthermore, almost nothing is known about the effects of CO_2 enrichment on photosynthesis and growth of the Raphidophycean flagellate *Chattonella*. In this study, the photosynthesis-irradiance (*P-E*) curves indicated that the maximum photosynthetic rate (P_{max}) and light-saturation parameter (E_k) were significantly higher under elevated CO_2 than under ambient CO_2 conditions in both species (Fig. 2). The P_{max} increased by about 78% for *C. marina* and 125% for *C. ovata*, as pCO_2 increased from 350 to 950 μatm. However, there were no significant differences in growth rates between pCO_2 levels or between species, although growth of both species seem to be higher under elevated pCO_2 than under ambient pCO_2 conditions (Fig. 3). These results appear to indicate that the cell growth and accumulation of

Chattonella are not affected by CO_2 enrichment, despite the increase in oxygen evolution rate being associated with high intercellular CO_2 concentrations. Why does the maximum photosynthetic rate (P_{max}) not result in increased growth of *Chattonella* under elevated CO_2 levels? The mechanisms responsible for this discrepancy are not clear but may be related to the activation of CCM, which facilitate active transport of CO_2 and / or HCO_3^- into the cytoplasm and chloroplast. With regard to the occurrence of a mechanism for energized transport of inorganic carbon, a number of CCM genes have been identified from de novo assembled transcriptomes in marine raphidophyte algae (Hennon et al. 2019). However, an essential feature of CCMs has yet to be confirmed with further experimental evidence of physiological mechanisms (Hennon and Dyhrman 2020, Raven et al. 2020). Some CCA genes, such as beta-carbonic anhydrases and a bicarbonate transporter, were significantly altered by both elevated CO_2 and growth rate, which is considered to be a response to down-regulation of CCM genes (Hennon et al. 2019). This suggests that raphidophytes may have the genetic capacity to use bicarbonate through its own CCM.

ACKNOWLEDGEMENTS

We would like to thank Professor Hae Jin Jeong for kindly offering *Chattonella ovata* strain and the Culture Collection of KIOST for providing *Chattonella marina* strain. This research was supported by a National Research Foundation (NRF) grant funded by the Korean government (MSIT) (NRF-2016R1A6A1A03012647, NRF-2020R1A2C3005053) to K.Y.K.

SUPPLEMENTARY MATERIALS

Supplementary Fig. S1. Continuous monitoring of temperatures for each temperature-controlled aquarium up to 10 d under ambient (A & B) and elevated pCO_2 (D & E) conditions for *Chattonella marina* and *C. ovata*, and an additional experiment for the growth rate of *C. marina* and *C. ovata* at the optimal growth temperature of 30°C under ambient and elevated pCO_2 (C & F) condition (https://e-algae.org).

Supplementary Fig. S2. Growth curves of *Chattonella marina* over time. Each point represents mean ± standard deviation (n = 3) for ambient (●) or elevated pCO_2 (▲) treatments in combination with 13, 20, 26, 30, or 34°C (https://e-algae.org).

Supplementary Fig. S3. Growth curves of *Chattonella ovata* over time. Each point represents mean ± standard deviation (n = 3) for ambient (●) or elevated pCO_2 (▲) treatments in combination with 13, 20, 26, 30, or 34°C (https://e-algae.org).

Supplementary Fig. S4. Maximum efficiency of photosystem II (PSII) photochemistry (F_v/F_m) of cultures at ambient (A & B) and elevated pCO_2 (C & D) levels for *Chattonella marina* and *C. ovata* at five temperatures (13, 20, 26, 30, 34°C) during the experiment. Error bars represent mean ± standard deviation (n = 3) (https://e-algae.org).

REFERENCES

Allakhverdiev, S. I., Kreslavski, V. D., Klimov, V. V., Los, D. A., Carpentier, R. & Mohanty, P. 2008. Heat stress: an overview of molecular responses in photosynthesis. Photosynth. Res. 98:541-550.

Angilletta, M. J. Jr. 2006. Estimating and comparing thermal performance curves. J. Therm. Biol. 31:541-545.

Beardall, J., Stojkovic, S. & Larsen, S. 2009. Living in a high CO_2 world: impacts of global climate change on marine phytoplankton. Plant Ecol. Divers. 2:191-205.

Bernhardt, J. R., Sunday, J. M., Thompson, P. L. & O'Connor, M. I. 2018. Nonlinear averaging of thermal experience predicts population growth rates in a thermally variable environment. Proc. R. Soc. B 285:20181076.

Bestion, E., Schaum, C. E. & Yvon-Durocher, G. 2018. Nutrient limitation constrains thermal tolerance in freshwater phytoplankton. Limnol. Oceanogr. Lett. 3:436-443.

Boatman, T. G., Lawson, T. & Geider, R. J. 2017. A key marine diazotroph in a changing ocean: the interacting effects of temperature, CO_2 and light on the growth of *Trichodesmium erythraeum* IMS101. PLoS ONE 12:e0168796.

Boyd, P. W., Rynearson, T. A., Armstrong, E. A., Fu, F., Hayashi, K., Hu, Z., Hutchins, D. A., Kudela, R. M., Litchman, E., Mulholland, M. R., Passow, U., Strzepek, R. F., Whittaker, K. A., Yu, E. & Thomas, M. K. 2013. Marine phytoplankton temperature versus growth responses from polar to tropical waters: outcome of a scientific community-wide study. PLoS ONE 8:e63091.

Brandenburg, K. M., Velthuis, M. & Van de Waal, D. B. 2019. Meta-analysis reveals enhanced growth of marine harmful algae from temperate regions with warming and elevated CO_2 levels. Glob. Chang. Biol. 25:2607-2618.

Clusella-Trullas, S., Blackburn, T. M. & Chown, S. L. 2011. Climatic predictors of temperature performance curve parameters in ectotherms imply complex responses to

climate change. Am. Nat. 177:738-751.

Core Writing Team, Pachauri, R. K. & Meyer, L. 2014. *Climate Change 2014: Synthesis Report. Contribution of Working Groups I, II and III to the Fifth Assessment Report of the Intergovernmental Panel on Climate Change*. IPCC, Geneva, 151 pp.

Coyne, K. J., Handy, S. M., Demir, E., Whereat, E. B., Hutchins, D. A., Portune, K. J., Doblin, M. A. & Cary, S. C. 2005. Improved quantitative real-time PCR assays for enumeration of harmful algal species in field samples using an exogenous DNA reference standard. Limnol. Oceanogr. Methods 3:381-391.

Daufresne, M., Lengfellner, K. & Sommer, U. 2009. Global warming benefits the small in aquatic ecosystems. Proc. Natl. Acad. Sci. U. S. A. 106:12788-12793.

Demura, M., Noël, M. -H., Kasai, F., Watanabe, M. M. & Kawachi, M. 2009. Taxonomic revision of *Chattonella antiqua*, *C. marina* and *C. ovata* (Raphidophyceae) based on their morphological characteristics and genetic diversity. Phycologia 48:518-535.

Dickson, A. G. 1993. The measurement of sea water pH. Mar. Chem. 44:131-142.

Eberlein, T., Van de Waal, D. B., Brandenburg, K. M., John, U., Voss, M., Achterberg, E. P. & Rost, B. 2016. Interactive effects of ocean acidification and nitrogen limitation on two bloom-forming dinoflagellate species. Mar. Ecol. Prog. Ser. 543:127-140.

Flynn, K. J., Clark, D. R., Mitra, A., Fabian, H., Hansen, P. J., Glibert, P. M., Wheeler, G. L., Stoecker, D. K., Blackford, J. C. & Brownlee, C. 2015. Ocean acidification with (de) eutrophication will alter future phytoplankton growth and succession. Proc. R. Soc. B 282:20142604.

Fu, F. X., Tatters, A. O. & Hutchins, D. A. 2012. Global change and the future of harmful algal blooms in the ocean. Mar. Ecol. Prog. Ser. 470:207-233.

García-Mendoza, E., Cáceres-Martínez, J., Rivas, D., Fimbres-Martinez, M., Sánchez-Bravo, Y., Vásquez-Yeomans, R. & Medina-Elizalde, J. 2018. Mass mortality of cultivated northern bluefin tuna *Thunnus thynnus orientalis* associated with *Chattonella* species in Baja California, Mexico. Front. Mar. Sci. 5:454.

Gattuso, J. -P., Gao, K., Lee, K., Rost, B. & Schulz, K. 2010. Approaches and tools to manipulate the carbonate chemistry. *In* Riebesell, U., Fabry, V. J., Hansson, L. & Gattuso, J. -P. (Eds.) *Guide to Best Practices for Ocean Acidification Research and Data Reporting*. Publications Office of the European Union, Luxembourg, pp. 41-52.

Gattuso, J. -P., Magnan, A., Billé, R., Cheung, W. W. L., Howes, E. L., Joos, F., Allemand, D., Bopp, L., Cooley, S. R., Eakin, C. M., Hoegh-Guldberg, O., Kelly, R. P., Pörtner, H.-O., Rogers, A. D., Baxter, J. M., Laffoley, D., Osborn, D., Rankovic, A., Rochette, J., Sumaila, U. R., Treyer, S. & Turley, C. 2015. Contrasting futures for ocean and society from different anthropogenic CO_2 emissions scenarios. Science 349:aac4722.

Genty, B., Briantais, J. -M. & Baker, N. R. 1989. The relationship between the quantum yield of photosynthesis electron transport and quenching of chlorophyll fluorescence. Biochim. Biophys. Acta Gen. Subj. 990:87-92.

Giordano, M., Beardall, J. & Raven, J. A. 2005. CO_2 concentrating mechanisms in algae: mechanisms, environmental modulation, and evolution. Annu. Rev. Plant Biol. 56:99-131.

Hallegraeff, G. M. 2010. Ocean climate change, phytoplankton community responses, and harmful algal blooms: a formidable predictive challenge. J. Phycol. 46:220-235.

Hazen, E. L., Jorgensen, S., Rykaczewski, R. R., Bograd, S. J., Foley, D. G., Jonsen, I. D., Shaffer, S. A., Dunne, J. P., Costa, D. P., Crowder, L. B. & Block, B. A. 2013. Predicted habitat shifts of Pacific top predators in a changing climate. Nat. Clim. Chang. 3:234-238.

Hennon, G. M. M. & Dyhrman, S. T. 2020. Progress and promise of omics for predicting the impacts of climate change on harmful algal blooms. Harmful Algae 91:101587.

Hennon, G. M. M., Williamson, O. M., Limón, M. D. H., Haley, S. T. & Dyhrman, S. T. 2019. Non-linear physiology and gene expression responses of harmful alga *Heterosigma akashiwo* to rising CO_2. Protist 170:38-51.

Imai, I. & Yamaguchi, M. 2012. Life cycle, physiology, ecology and red tide occurrences of the fish-killing raphidophyte *Chattonella*. Harmful Algae 14:46-70.

Jeong, H. J. 2011. Mixotrophy in red tide algae Raphidophytes. J. Eukaryot. Microbiol. 58:215-222.

Jeong, H. J., Seong, K. A., Kang, N. S., Yoo, Y. D., Nam, S. W., Park, J. Y., Shin, W., Glibert, P. M. & Johns, D. 2010. Feeding by raphidophytes on the cyanobacterium *Synechococcus* sp. Aquat. Microb. Ecol. 58:181-195.

Jeong, H. J., Yoo, Y. D., Lim, A. S., Kim, T. -W., Lee, K. & Kang, C. K. 2013. Raphidophyte red tides in Korean waters. Harmful Algae 30(Suppl. 1):S41-S52.

Jin, P. & Agustí, S. 2018. Fast adaptation of tropical diatoms to increased warming with trade-offs. Sci. Rep. 8:17771.

Kahn, S., Arakawa, O. & Onoue, Y. 1998. Physiological investigations of a neurotoxin-producing phytoflagellate, *Chattonella marina* (Raphidophyceae). Aquac. Res. 29:9-17.

Kibler, S. R., Tester, P. A., Kunkel, K. E., Moore, S. K. & Litaker, R. W. 2015. Effects of ocean warming on growth and distribution of dinoflagellates associated with ciguatera fish poisoning in the Caribbean. Ecol. Modell. 316:194-

210.

Kim, J. -H., Kang, E. J., Kim, K. & Kim, K. Y. 2018. A continuous-flow and on-site mesocosm for ocean acidification experiments on benthic organisms. Algae 33:359-366.

Kim, S. Y., Seo, K. S., Lee, C. G. & Lee, Y. 2007. Diurnal modification of a red-tide causing organism, *Chattonella antiqua* (Raphidophyceae) from Korea. Algae 22:95-106.

Kingsolver, J. G. 2009. The well-temperatured biologist (American Society of Naturalists presidential address). Am. Nat. 174:755-768.

Kontopoulos, D. -G., Van Sebille, E., Lange, M., Yvon-Durocher, G., Barraclough, T. G. & Pawar, S. 2020. Phytoplankton thermal responses adapt in the absence of hard thermodynamic constraints. Evolution 74:775-790.

Kremp, A., Godhe, A., Egardt, J., Dupont, S., Suikkanen, S., Casabianca, S. & Penna, A. 2012. Intraspecific variability in the response of bloom-forming marine microalgae to changed climate conditions. Ecol. Evol. 2:1195-1207.

Lewis, E. R. & Wallace, D. W. R. 1998. *Program developed for CO_2 system calculations*. Carbon Dioxide Information Center. Oak Ridge National Laboratory, U.S. Department of Energy, Oak Ridge, 38 pp.

Lewitus, A. J., Brock, L. M., Burke, M. K., De Mattio, K. A. & Wilde, S. B. 2008. Lagoonal stormwater detention ponds as promoters of harmful algal blooms and eutrophication along the South Carolina coast. Harmful Algae 8:60-65.

Marshall, J. A. & Hallegraeff, G. M. 1999. Comparative ecophysiology of the harmful alga *Chattonella marina* (Raphidophyceae) from South Australian and Japanese waters. J. Plankton Res. 21:1809-1822.

Millero, F. J., Zhang, J. -Z., Lee, K. & Campbell, D. M. 1993. Titration alkalinity of seawater. Mar. Chem. 44:153-165.

Noh, I. H. 2009. Physiological and ecological studies on the harmful algae *Chatttonella* spp. (Raphidophyceae) in the coastal waters of Korea. Ph.D. dissertation, Chonnam National University, Gwangju, Korea, 130 pp.

Onitsuka, G., Yamaguchi, M., Sakamoto, S., Shikata, T., Nakayama, N., Kitatsuji, S., Itakura, S., Sakurada, K., Ando, H., Yoshimura, N., Mukai, H. & Yamashita, H. 2020. Interannual variations in abundance and distribution of *Chattonella* cysts, and the relationship to population dynamics of vegetative cells in the Yatsushiro Sea, Japan. Harmful Algae 96:101833.

Platt, T., Gallegos, C. L. & Harrison, W. G. 1980. Photoinhibition of photosynthesis in natural assemblages of marine phytoplankton. J. Mar. Res. 38:687-701.

Qiu, X., Mukai, K., Shimasaki, Y., Wu, M., Chen, C., Lu, Y., Ichinose, H., Nakashima, T., Kato-Unoki, Y. & Oshima, Y. 2020. Diurnal variations in expression of photosynthesis-related proteins in the harmful Raphidophyceae *Chattonella marina* var. *antiqua*. J. Exp. Mar. Biol. Ecol. 527:151361.

Raven, J. A. 2017. The possible roles of algae in restricting the increase in atmospheric CO_2 and global temperature. Eur. J. Phycol. 52:506-522.

Raven, J. A., Gobler, C. J. & Hansen, P. J. 2020. Dynamic CO_2 and pH levels in coastal, estuarine, and inland waters: theoretical and observed effects on harmful algal blooms. Harmful Algae 91:101594.

Rosso, L., Lobry, J. R., Bajard, S. & Flandrois, J. P. 1995. Convenient model to describe the combined effects of temperature and pH on microbial growth. Appl. Environ. Microbiol. 61:610-616.

Rosso, L., Lobry, J. R. & Flandrois, J. P. 1993. An unexpected correlation between cardinal temperatures of microbial growth highlighted by a new model. J. Theor. Biol. 162:447-463.

Rost, B., Zondervan, I. & Wolf-Gladrow, D. 2008. Sensitivity of phytoplankton to future changes in ocean carbonate chemistry: current knowledge, contradictions and research directions. Mar. Ecol. Prog. Ser. 373:227-237.

Satta, C. T., Padedda, B. M., Sechi, N., Pulina, S., Loria, A. & Lugliè, A. 2017. Multiannual *Chattonella subsalsa* Biecheler (Raphidophyceae) blooms in a Mediterranean lagoon (Santa Giusta Lagoon, Sardinia Island, Italy). Harmful algae 67:61-73.

Schulz, K., Barcelos e Ramos, J., Zeebe, R. E. & Riebesell, U. 2009. CO_2 perturbation experiments: similarities and differences between dissolved inorganic carbon and total alkalinity manipulations. Biogeosciences 6:2145-2153.

Seto, D. S., Karp-Boss, L. & Wells, M. L. 2019. Effects of increasing temperature and acidification on the growth and competitive success of *Alexandrium catenella* from the Gulf of Maine. Harmful Algae 89:101670.

Shikata, T., Takahashi, F., Nishide, H., Shigenobu, S., Kamei, Y., Sakamoto, S., Yuasa, K., Nishiyama, Y., Yamasaki, Y. & Uchiyama, I. 2019. RNA-seq analysis reveals genes related to photoreception, nutrient uptake, and toxicity in a noxious red-tide raphidophyte *Chattonella antiqua*. Front. Microbiol. 10:1764.

Singh, S. P. & Singh, P. 2015. Effect of temperature and light on the growth of algae species: a review. Renew. Sustain. Energy Rev. 50:431-444.

Stacca, D., Satta, C. T., Casabianca, S., Penna, A., Padedda, B. M., Sechi, N. & Lugliè, A. 2016. Identification of *Chattonella* (Raphidophyceae) species in long-term phytoplankton samples from Santa Giusta Lagoon, Italy. Sci. Mar. 80:17-25.

Tatters, A. O., Roleda, M. Y., Schnetzer, A., Fu, F., Hurd, C. L., Boyd, P. W., Caron, D. A., Lie, A. A. Y., Hoffman, L. J. & Hutchins, D. A. 2013. Short and long-term conditioning of temperate marine diatom community to acidification and warming. Philos. Trans. R. Soc. B 368:20120437.

Thomas, M. K., Aranguren-Gassis, M., Kremer, C. T., Gould, M. R., Anderson, K., Klausmeier, C. A. & Litchman, E. 2017. Temperature-nutrient interactions exacerbate sensitivity to warming in phytoplankton. Glob. Chang. Biol. 23:3269-3280.

Thomas, M. K., Kremer, C. T., Klausmeier, C. A. & Litchman, E. 2012. A global pattern of thermal adaptation in marine phytoplankton. Science 338:1085-1088.

Thomas, M. K., Kremer, C. T. & Litchman, E. 2016. Environment and evolutionary history determine the global biogeography of phytoplankton temperature traits. Glob. Ecol. Biogeogr. 25:75-86.

Thoms, S., Pahlow, M. & Wolf-Gladrow, D. A. 2001. Model of the carbon concentrating mechanism in chloroplasts of eukaryotic algae. J. Theor. Biol. 208:295-313.

Tilney, C. L., Hoadley, K. D. & Warner, M. E. 2015. Comparing the diel vertical migration of *Karlodinium veneficum* (Dinophyceae) and *Chattonella subsalsa* (Raphidophyceae): PSII photochemistry, circadian control, and carbon assimilation. J. Photochem. Photobiol. B 143:107-119.

Tortell, P. D., Rau, G. H. & Morel, F. M. M. 2000. Inorganic carbon acquisition in coastal Pacific phytoplankton communities. Limnol. Oceanogr. 45:1485-1500.

Van de Waal, D. B., Brandenburg, K. M., Keuskamp, J., Trimborn, S., Rokitta, S., Kranz, S. A. & Rost, B. 2019. Highest plasticity of carbon-concentrating mechanisms in earliest evolved phytoplankton. Limnol. Oceanogr. Lett. 4:37-43.

Vidyarathna, N. K., Papke, E., Coyne, K. J., Cohen, J. H. & Warner, M. E. 2020. Functional trait thermal acclimation differs across three species of mid-Atlantic harmful algae. Harmful Algae 94:101804.

Vrieling, E. G., Koeman, R. P. T., Nagasaki, K., Ishida, Y., Pererzak, L., Gieskes, W. W. C. & Veenhuis, M. 1995. *Chattonella* and *Fibrocapsa* (Raphidophyceae): first observation of, potentially harmful, red tide organisms in Dutch coastal waters. Neth. J. Sea Res. 33:183-191.

Wang, B., Wu, D., Chu, K. H., Ye, L., Yip, H. Y., Cai, Z. & Wong, P. K. 2017. Removal of harmful alga, *Chattonella marina*, by recyclable natural magnetic sphalerite. J. Hazard. Mater. 324:498-506.

Wang, Z. -H., Qi, Y. -Z., Chen, J. -F. & Xu, N. 2006. Population dynamics of *Chattonella* in spring in Daya Bay, the South China Sea and the cause of its blooms. Acta Hydrobiol. Sin. 30:394-398.

Watanabe, M., Kohata, K. & Kimura, T. 1991. Diel vertical migration and nocturnal uptake of nutrients by *Chattonella antiqua* under stable stratification. Limnol. Oceanogr. 36:593-602.

Yamaguchi, H., Mizushima, K., Sakamoto, S. & Yamaguchi, M. 2010. Effects of temperature, salinity and irradiance on growth of the novel red tide flagellate *Chattonella ovata* (Raphidophyceae). Harmful Algae 9:398-401.

Yamaguchi, H., Tanimoto, Y., Hayashi, Y., Suzuki, S., Yamaguchi, M. & Adachi, M. 2018. Bloom dynamics of noxious *Chattonella* spp. (Raphidophyceae) in contrastingly enclosed coastal environments: a comparative study of two coastal regions. J. Mar. Biol. Assoc. U. K. 98:657-663.

Yamochi, S. 1984. Effects of temperature on the growth of six species of red-tide flagellates occurring in Osaka Bay. Bull. Plankton Soc. Jpn. 3l:5-22.

Yoshimatsu, S. & Ono, C. 1986. The seasonal appearance of the red tide organisms and flagellates in the southern Harima-Nada, Inland Sea of Seto. Bull. Akashiwo Res. Inst. Kagawa Pref. 2:1-42.

Zhang, Y., Fu, F. -X., Whereat, E., Coyne, K. J. & Hutchins, D. A. 2006. Bottom-up controls on a mixed-species HAB assemblage: a comparison of sympatric *Chattonella subsalsa* and *Heterosigma akashiwo* (Raphidophyceae) isolates from the Delaware Inland Bays, USA. Harmful Algae 5:310-320.

Zingone, A., Escalera, L., Aligizaki, K., Fernández-Tejedor, M., Ismael, A., Montresor, M., Mozetič, P., Taş, S. & Totti, C. 2020. Toxic marine microalgae and noxious blooms in the Mediterranean Sea: a contribution to the Global HAB Status Report. Harmful Algae. Advanced online publication. https://doi.org/10.1016/j.hal.2020.101843.